

Elsevier required licence: © 2021

This manuscript version is made available under the
CC-BY-NC-ND 4.0 license

<http://creativecommons.org/licenses/by-nc-nd/4.0/>

The definitive publisher version is available online at

<https://doi.org/10.1016/j.desal.2021.115196>

1 **Submerged versus side-stream osmotic membrane bioreactors using an outer-selective**
2 **hollow fiber osmotic membrane for desalination**

3 Van Huy Tran¹, Sungil Lim^{1,2}, Paula Jungwon Choi³, Alicia Kyoungjin An³, Dong Suk Han⁴,
4 Sherub Phuntsho¹ and Hokyong Shon^{1*}

5
6
7 *¹Centre for Technology in Water and Wastewater (CTWW), School of Civil and Environmental*
8 *Engineering, University of Technology Sydney (UTS), Australia*

9 *²Environment Systems Research Division, Korea Institute of Machinery and Materials (KIMM),*
10 *Daejeon, Republic of Korea*

11 *³School of Energy and Environment, City University of Hong Kong, Tat Chee Avenue, Kowloon,*
12 *Hong Kong, China*

13 *⁴Center for Advanced Materials, Qatar University, P.O. Box 2713, Doha, Qatar*

14
15
16
17
18
19
20
21
22
23

* Corresponding author: Prof. Hokyong Shon Email: hokyong.shon-1@uts.edu.au.

24 **Abstract**

25 This study investigated the comparative performances, fouling mitigation efficiencies, and
26 operational costs of side-stream and submerged osmotic membrane bioreactors (OMBR)
27 systems using an outer-selective hollow fiber thin-film composite forward osmosis (OSHF
28 TFC FO) membrane. Generally, the submerged OMBR system exhibited the higher fouling
29 mitigation efficiency and a much slower flux decline rate when compared with that of the side-
30 stream system. The side-stream OMBR system demonstrated an initial water flux of 15.8 LMH
31 using 35 g/L NaCl as the draw solution, which was 2-fold higher than that of the submerged
32 system when at its optimal performance. However, salinity accumulation in the reactor of the
33 side-stream system was at a higher rate than for the submerged OMBR system. Both OMBR
34 systems showed comparably high pollutant removal efficiencies over the experimental period.
35 Annual operating costs for the side-stream OMBR system has been estimated to be 38% higher
36 (OPEX) than for the submerged system. Membrane replacement cost accounted for the
37 majority of the OPEX, over 89%, while the energy consumption and cleaning costs only
38 accounted for relatively small portions. Therefore, reducing the membrane replacement cost is
39 critical to realizing the commercial viability of the submerged OMBR system.

40

41

42

43 **Keywords:** *Submerged module, Side-stream module, Outer-selective hollow fiber; Membrane*
44 *fouling, Operating cost, Osmotic membrane bioreactor.*

45

46 **1 Introduction**

47 Osmotic membrane bioreactors (OMBR) have recently attracted significant research interests for
48 use in wastewater reclamation and desalination applications [1, 2]. While many of obvious
49 advantages (i.e., high quality permeate, suitable for nutrient recovery) have been confirmed by
50 previous OMBR studies [3], membrane fouling still remains a key concern [4-6]. Membrane
51 fouling is an unavoidable issue in any membrane filtration processes, causing water flux and water
52 quality to decline and may also reduce membrane lifetime, requiring more frequent cleaning and
53 replacement, thereby increasing operational cost [7]. Therefore, effective fouling mitigation
54 methods are essential to maintain a sustainable operation of forward osmosis (FO) processes and
55 OMBR system. Recently, membrane fouling strategies have been assessed, including:
56 investigation of suitable protocols for effective membrane cleaning methods; optimization of
57 operating parameters related to membrane fouling including operating flux, draw solution (DS)
58 properties, membrane orientation, optimum cross-flow velocity (CFV), specific aeration demand
59 (SAD); and the application of high anti-fouling membranes and creative membrane and membrane
60 module configuration designs. [8].

61 A large number of recent OMBR studies have applied flat-sheet membrane module as their main
62 configuration [2, 3, 7, 9-12] while comparatively fewer studies have utilized FO membranes with
63 hollow configurations [13-15]. As for the hollow fiber FO membrane, the polyamide selective
64 layer can be coated either on the lumen side, which is called inner selective hollow fiber (ISHF),
65 or on the outer surface of the fiber to form an outer-selective hollow fiber (OSHF). Whilst Zhang
66 et.al [13] have used ISHF FO membranes for their OMBR study, Tran et. al [14] applied an OSHF
67 FO membrane to investigate the fouling mitigation efficacy of the OMBR system. Compared to
68 ISHF membranes, OSHF membranes offer several merits, including larger membrane surface area,

69 lower fouling potential, and easier cleaning under the active layer facing FS (AL-FS) orientation
70 [16-18]. When the ISHF FO membrane is used under the AL-FS orientation, FS (activated sludge)
71 is recirculated on the lumen side of the fiber, which can cause severe clogging and blocking inside
72 the micro-sized hollow fiber due to the suspended flocs, particulates, and foulants present. Under
73 this membrane orientation, the OSHF FO membrane is more suitable as the FS is circulated outside
74 of the fiber, and therefore not only prevents clogging and blockage inside the fiber, but also offers
75 a more favorable condition for membrane cleaning. As fouling occurs, a fouling-cake layer can be
76 formed on the outer surface of the fiber which can be easily and effectively mitigated by physical
77 cleaning (i.e., using high shear force generated by elevated CFV), air scouring, and/or chemical
78 cleaning.

79 Side-stream (external cross-flow) modules and submerged (plate-and-frame) modules are the two
80 main configurations in which submerged modules have been widely applied for both conventional
81 MBR and OMBR studies [9, 19]. In the external cross-flow module, activated sludge flows through
82 the membrane module and is recirculated back to the bioreactor while the submerged module is
83 directly immersed into the bioreactor, and therefore, in direct contact with the activated sludge.
84 The application of the external cross-flow module in OMBR systems is expected to provide
85 favorable conditions for controlling membrane fouling and reducing the effect of external
86 concentration polarization (ECP) by simply enhancing the CFV of the FS stream. Also, chemical
87 cleaning can be carried out in-place (CIP) in the side-stream module with minimum interruption
88 and downtime. Nonetheless, the disadvantages of side-stream OMBR system is the high
89 operational cost due to the additional pumping energy required for the activated sludge. Further,
90 the strong pumping shear could break the flocs formed in the bioreactor resulting in a lower sludge
91 yield and reduced chemical oxygen demand (COD) removal rate [20].

92 Submerged OMBR systems do not require circulation of activated sludge, thereby eliminating the
93 pumping energy and also the adverse impact on microorganism growth and treatment activities
94 [20]. Although the fouling potential of submerged MBR system is higher than the crossflow side-
95 stream system, however, submerged OMBR systems can utilize the air bubbles used for aeration
96 as a measure of continuous air scouring to minimize fouling and ECP mitigation [9, 21].
97 Nevertheless, CIP is not feasible for submerged OMBR and membrane cleaning will definitely
98 require the interruption of the system's operation.

99 Application of external cross-flow (side-stream) or submerged membrane modules for OMBR
100 systems has both pros and cons that significantly influence the fouling mitigation efficacy and
101 overall system performance. It is therefore essential to systematically investigate and compare the
102 performance of these two OMBR system configurations. This study aims to evaluate and compare
103 the fouling mitigation efficiency and operational costs of the two OMBR systems using side-
104 stream and submerged membrane modules. Performance was assessed based on water flux, salt
105 accumulation in the activated sludge, and the pollutant removal efficacy. Fouling mitigation
106 efficiency was evaluated according to the flux decline rate over the testing period and flux recovery
107 after the implementation of a fouling cleaning method. Membrane autopsies were then conducted
108 on the fouled membranes with a scanning electron microscope (SEM) and an energy diffusive X-
109 ray (EDX) to obtain the surface and cross-sectional morphologies, and the elemental compositions
110 of fouling cake-layer for a better understanding of the membrane fouling and the mitigation
111 efficacy.

112

113 **2 Materials and methods**

114 **2.1 Side-stream and submerged membrane module.**

115 This study used submerged and side-stream modules with the same membrane surface areas,
116 comprised of OSHF TFC FO membranes, fabricated and developed at the Center for Technology
117 in Water and Wastewater, University of Technology Sydney, Australia. Specifications of the lab-
118 scale side-stream and submerged membrane modules are described in **Fig. S1** and **Table S1**. The
119 property of the OSHF TFC FO membrane have also described elsewhere in our previous studies
120 [14, 22].

121 **2.2 Draw solution and synthetic wastewater.**

122 The chemicals used were all of reagent grade, supplied by Merck, Australia. Sodium chloride
123 (NaCl) solution with a concentration of 35 g/L was used as the DS. Synthetic wastewater was
124 prepared using the same recipe as the one described in our previous study [14].

125 **2.3 Experiment protocols**

126 **2.3.1 Experiment setup for baseline tests**

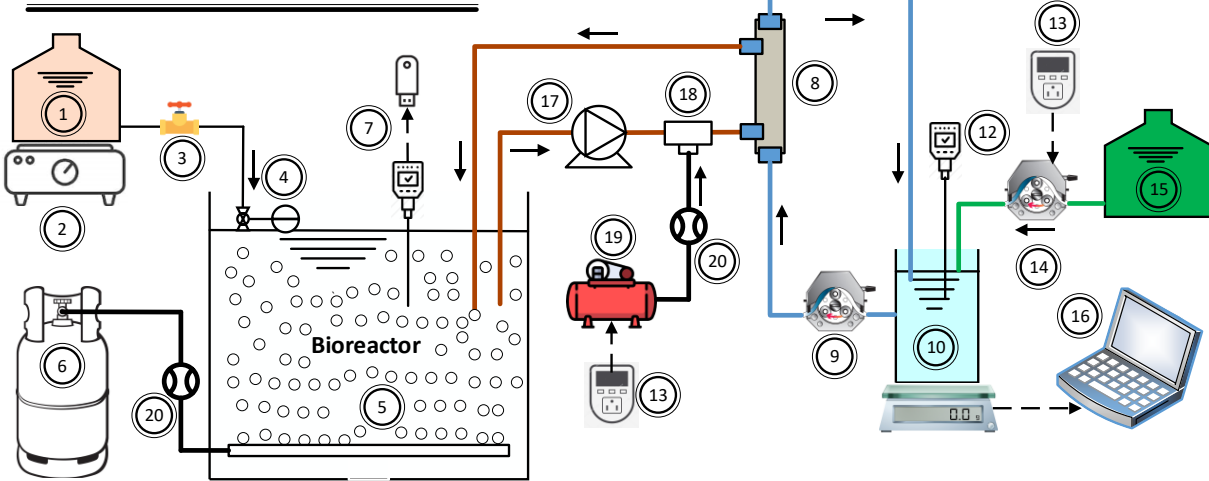
127 Schematics of the FO testing systems for the side-stream and submerged membrane modules are
128 depicted in **Fig. S2**. The objective of these tests was to verify the performance of each module
129 before installation into the OMBR systems to allow for comparison of the performance of the two
130 membrane module configurations. These tests used sodium chloride (NaCl) solution with a
131 concentration of 35 g/L as DS and deionized (DI) water as the FS. Water flux (J_w) and specific
132 reverse solute flux (SRSF) were two main parameters used for verifying modules' performance.
133 Testing conditions are tabulated in **Table. S2**.

134 **2.4 The bench-scale submerged and side-stream OMBR systems**

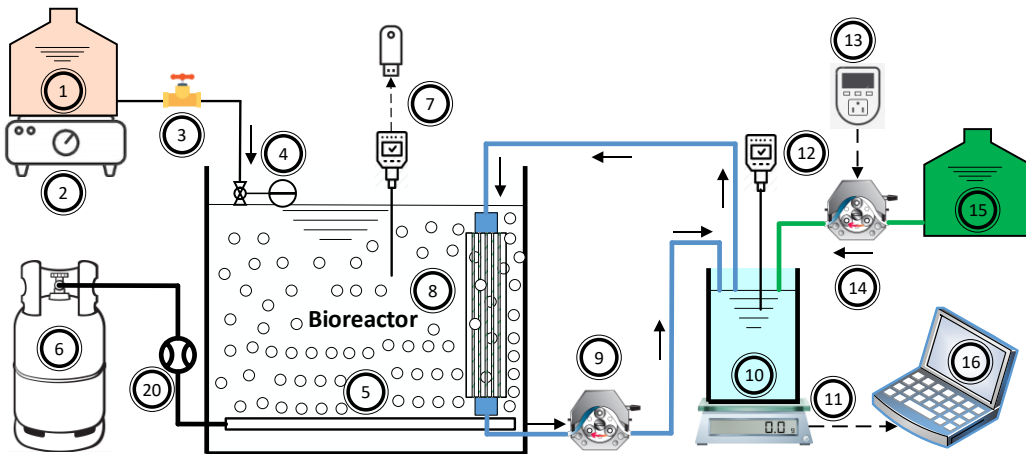
135 This research work used two lab-scale OMBR systems, with side-stream and submerged

136 membrane modules, as depicted in **Fig. 1**.

(a) Side-stream OMBR testing system



(b) Submerged OMBR testing system



- | | | | |
|--------------------|--------------------------|-------------------------|---------------------------|
| ① Wastewater tank | ⑥ Air Cylinder | ⑪ Balance | ⑯ Laptop for data logging |
| ② Magnetic stirrer | ⑦ Conductivity, pH meter | ⑫ Conductivity meter | ⑰ Gear pump |
| ③ Closing valve | ⑧ Membrane module | ⑬ Timer switch | ⑱ Connecting Tee |
| ④ Float valve | ⑨ Peristaltic pump | ⑭ Peristaltic pump | ⑲ Air pump |
| ⑤ Air diffuser | ⑩ Draw solution tank | ⑮ 5M NaCl solution tank | ⑳ Air flow meter |

138 **Figure 1.** Bench-scale OMBR systems using side-stream and submerged membrane modules.

139 2.4.1 **Operations of submerged and side-stream OMBR systems**

140

141 The two OMBR systems in this study employed acclimatized activated sludge obtained from the
142 water recycling facility at Sydney Central Park. Before being used for the experiments, activated
143 sludge was acclimatized for more than 6 months, until the achieved TOC removal efficiency was
144 consistently over 90%. A volume of 1.5 L with a mixed liquor suspended solids (MLSS)
145 concentration of 6.5 ± 0.2 g/L, and total dissolved solids (TDS) of 0.53 ± 0.05 g/L was poured into
146 the reactor of each OMBR system. A floating valve was installed in the reactor of each system to
147 control the incoming volume of synthetic wastewater influent and to maintain a constant water
148 level in the reactor. An air diffuser (Aqua One, Australia) was employed in each OMBR system
149 reactor to provide aeration with an intensity of 3 L/min, maintaining the dissolved oxygen
150 concentration in the bioreactor at a level of more than 3 mg/L for microorganisms. A portable pH
151 and conductivity meter - HQ40D (HACH, Germany) was used in each system to regularly monitor
152 the salinity and pH of the activated sludge in each reactor.

153 DS was recirculated from the membrane modules back to the DS tank by a peristaltic pump
154 (LongerPump, USA). For the submerged OMBR system, DS was circulated at a flowrate of 10
155 ml/min through the submerged membrane module in sucking mode (the submerged module was
156 connected to the suction line of the pump). Regarding the side-stream OMBR system, DS was
157 pumped at a flowrate of 21 ml/min into the cross-flow module under the pushing mode, (side-
158 stream module was connected to the pushing line of the pump). A DS concentration-controlling
159 unit, including a conductivity probe and a programmable timer switch connected to a peristaltic
160 dosing pump (LongerPump, USA) was used for maintaining a constant DS concentration at $35 \pm$

161 1 g/L by automatically supplementing a highly concentrated (5M) NaCl stock solution into the DS
162 tank. As for the side-stream OMBR system, a gear pump (Cole-Parmer, USA) was used to circulate
163 the activated sludge at a flowrate of 1 L/min from the reactor to the side-stream module which was
164 then returned to the reactor. The solid retention time (SRT) was maintained at 30 days for both
165 OMBR systems, with a daily discharge of 50 ml of mixed liquor. As for the side-stream OMBR
166 system, aeration of 3 L/min was injected together with the cross-flow of the activated sludge to
167 the membrane module for 5 minutes every two hours as a fouling mitigation method. All
168 experiments were conducted in the laboratory, under a highly controlled environment with an
169 ambient temperature of $22 \pm 1^\circ\text{C}$.

170 Daily physical cleaning was applied to the side-stream membrane module for 15 minutes over the
171 course of the experiment. Physical cleaning involved a crossflow circulation of DI water into the
172 side-stream module at 1.5 L/min with simultaneous aeration at 3 L/min to remove any fouling cake
173 layer that may have formed on the outer surface of the hollow fiber membrane. Physical cleaning
174 was also applied to the submerged module only when water flux dropped by 40% since the surface
175 of the submerged membrane was in constant contact with air bubbles in the submerged OMBR
176 system. The submerged membrane module was removed from the system and was installed in a
177 cleaning tank containing DI water with continuous aeration at a rate of 3 L/min for 15 minutes.

178 **2.5 Analytical methods**

179 **2.5.1 Determination of water flux and specific reverse solute flux**

180 Water flux - J_w ($\text{L}/\text{m}^2 \text{ h}$ - LMH) was calculated by Equation [1]:

$$181 \quad J_w = \frac{\Delta V}{A_m \times \Delta t} \quad [1]$$

182 Where: A_m (m^2) is an effective area of FO membrane; Δt (h) is time interval; ΔV is the net volume
183 change of DS solution (L). When DI water is used as FS, reverse solute flux - J_s ($g/m^2 h - gMH$)
184 was calculated using Equation [2]:

$$185 \quad J_s = \frac{\Delta V \times \Delta C_t}{A_m \times \Delta t} \quad [2]$$

186 Where: ΔV and ΔC_t are the net changes in the FS volume (L) and FS's salt concentration; Δt (h)
187 and A_m (m^2) are the same as in Equation [1]. Subsequently, the specific reverse solute flux (SRSF)
188 was determined by Equation [3]:

$$189 \quad SRSF = \frac{J_s}{J_w} \quad [3]$$

190 2.5.2 Determination of water quality parameters and pollutant removal efficiency

191 COD, MLSS, and mixed liquor volatile suspended solids (MLVSS) were measured according to
192 standardized methods for the examination of water and wastewater [23]. Measurement of dissolved
193 oxygen (DO) was carried out using a DO meter (Vernier, USA). Samples were regularly collected
194 from the synthetic wastewater tank, the reactor, and the DS tank for analysis of the basic pollutant
195 concentrations. Measurements of TOC concentrations in the collected samples were carried out
196 using the TOC analyzer (Multi N/C 2000, Analytik Jena GmbH, Germany). Concentrations of
197 NH_4^+ , TN, and PO_4^{3-} were measured using the corresponding test kits and photometer -
198 Spectroquant, NOVA 60 (Merck, Australia). In order to attain accurate analytical values, samples
199 were pretreated, followed by dilution, if necessary, to minimize the interference of chloride and to
200 ensure the proper range of analytes. Pollutant removal efficiencies (R_{eff}) of the OMBR systems
201 were calculated using the following equations:

$$202 \quad R_{eff}(\%) = \left(1 - \frac{C_{DS} \times DF}{C_{ww}}\right) \times 100 \quad [4]$$

203 where C_{DS} and C_{ww} are the concentrations of pollutants in mg/L of draw solution and synthetic
204 wastewater, respectively. DF is the dilution factor taking into account the volume of permeate,
205 which is calculated by Equation [5].

$$206 \quad DF = \left(1 + \frac{V_{Per}}{V_{DS}^i} \right) \quad [5]$$

207 where V_{DS}^i and V_{Per} are, respectively, the initial volume of DS volume of permeated water through
208 the FO membrane at the time when samples are collected.

209 **2.6 Membrane and fouling cake layer characterization**

210 Fouled membrane samples were taken from the submerged and cross-flow module at the end of
211 each experiment for analysis of their morphological structures and elemental compositions.
212 Samples were dried at ambient temperature ($22 \pm 1^\circ\text{C}$) before being coated with platinum in a high
213 vacuum sputter coater (EM ACE600, Leica). Subsequently, membrane samples were analyzed in
214 a field emission scanning microscopy and an energy diffusive X-ray (EDX) analyzer (FE-SEM,
215 Zeiss Supra 55VP, Carl Zeiss AG).

216 **2.7 Operating cost analysis**

217 Operating costs (OPEXs) of the two OMBR systems were estimated and analyzed for economic
218 comparison between the two OMBR membrane module configurations. The boundary of the
219 OPEX calculation is presented in **Fig. S3**. OPEXs were calculated based on the following
220 considerations and assumptions:

- 221 ▪ OPEX cost were calculated assuming full-scale OMBR systems with the same capacity of
222 24,000 m³/day, with effluent from both OMBR systems having a similar TDS of 3.6 ± 0.1
223 g/L.
- 224 ▪ OPEXs in this study were comprised three main costs components: energy consumption
225 (EC); membrane replacement (MR); and cleaning chemicals (CC).

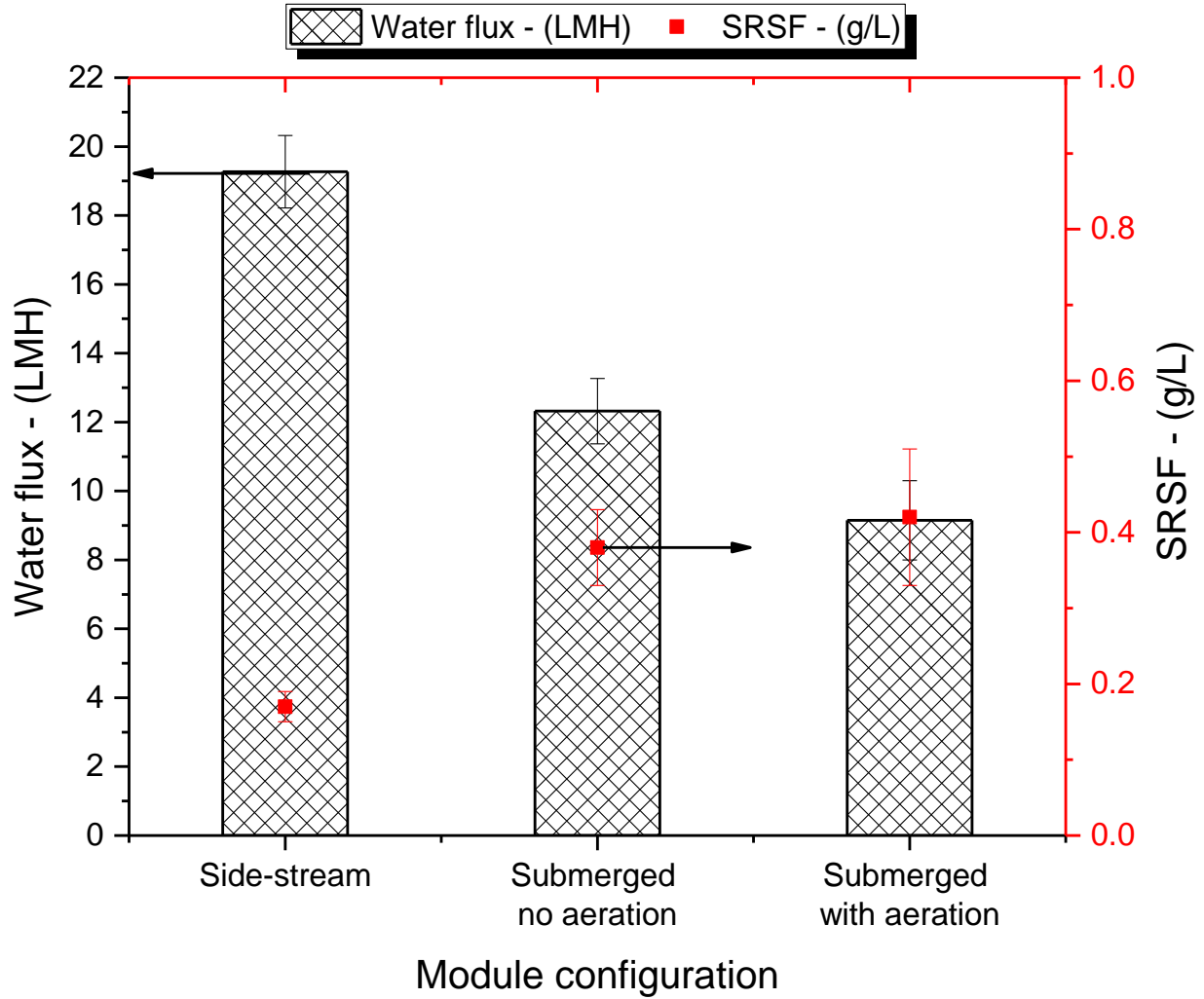
- 226 ▪ EC costs included pumping energy for the circulation of FS and regular injection of air
227 bubbles into the membrane module (for the side-stream OMBR system only) and DS
228 pumping for both OMBR systems. MR cost is calculated with an assumed lifetime of 7
229 years for submerged membrane module and 5 years for side-stream membrane module,
230 (membrane lifetime is reduced because of additional shear force and high CFV with
231 pressure in the side-stream module). CC cost includes energy consumption for pumping
232 water, recirculating water during physical and chemical cleaning processes, air pumps,
233 water cost, and the chemical costs for NaOH and citric acid.
- 234 ▪ OPEX cost calculation in this study excludes the following costs: construction,
235 infrastructure system, accessories, transport, used membranes, maintenance costs, aeration
236 cost for maintaining dissolved oxygen for microorganism, and waste management.
- 237 ▪ Energy costs were calculated assuming an electricity price of AU \$0.29/kWh [24], a water
238 price of AU \$1.97/1kL, prices of NaOH and Citric acid are AU \$100/ton and AU \$840/ton,
239 respectively.
- 240 ▪ The costs of the outer selective hollow fiber FO membrane module were assumed to be
241 AU \$1,250 for the side-stream membrane module [24], and AU \$625 for the submerged
242 one. The higher cost for the side-stream membrane module is due to the costs for housing
243 materials and the additional complexity in production. Specifications of the assumed
244 commercial membrane modules are presented in Table S3.
- 245 ▪ Average water fluxes, used for calculation of operational cost, were taken from the
246 performance of each membrane module in each OMBR system.

- 247 ▪ Daily physical cleaning is assumed to be applied to the side-stream membrane module, and
248 a fortnightly physical cleaning is applied to the submerged membrane module. A quarterly
249 chemical cleaning is carried out for both side-stream and submerged membrane modules.
- 250 ▪ Chemical cleaning was assumed to be performed with an alkaline-acidic cleaning protocol
251 for both the submerged and side-stream membrane modules. Initially, physical cleaning
252 using clean water and aeration with an intensity of 3 L/min was carried out for 5 minutes.
253 Next, NaOH solution (0.1% w/v, at pH 12) was then used for alkaline cleaning for 30
254 minutes. The first step was then repeated for 5 minutes. Subsequently, acidic cleaning was
255 carried out using a citric acid solution (2% w/v, pH 3) for 30 minutes. Finally, the first step
256 was repeated for 5 minutes for cleaning the membrane module and remove residual of the
257 citric acid solution before membrane modules are brought back to operation.

258

259 **3 Results and discussion**

260 **3.1 Baseline performance of side-stream and submerged modules**



261

262 **Figure 2.** Performance (J_w and SRSF) of the OSHF TFC FO membrane module with side-stream
263 and submerged configurations. Testing conditions: FS = DI water; DS = 35 g/L NaCl; AL – FS
264 orientation; Ambient temperature ($22 \pm 1^\circ\text{C}$).

265 **Fig. 2** shows the performance (J_w and SRSF) of the two membrane modules under cross-flow and
266 submerged configurations using the OSHF TFC FO membrane under the initial test with DI water

267 as FS. As clearly indicated in the figure, the side-stream module exhibited higher water flux (19.3
268 LMH) and an SRSF (0.17 g/L) when compared to the submerged membrane module with a J_w of
269 12.3 LMH and an SRSF of 0.38 g/L. This result is in agreement with the one observed by Blandin
270 et. al [25] in their performance comparison of submerged and cross-flow membrane modules using
271 a flat-sheet TFC FO membrane. The lower performance of the submerged membrane module could
272 be ascribed to a more severe concentrative external concentration polarization (CECP) effect on
273 the submerged system. Different operating conditions between the two systems resulted in distinct
274 hydrodynamic behaviors in each system, which resulted in the dissimilar CECP effects. Moreover,
275 recirculation of FS inside the side-stream module with a CFV generated turbulence and a shear
276 force on the outer surface of each fiber, mitigating the severity of the CECP effect. As for the
277 submerged system, while stirring was carried out in the FS tank, the effectiveness of CECP
278 mitigation might not be as high as that in the side-stream system because less shear force and
279 turbulence were made under the absence of CFV. CECP is therefore likely to be a more serious
280 nearby the outer surface of hollow fiber where the reverse diffusion of draw solutes occurs.

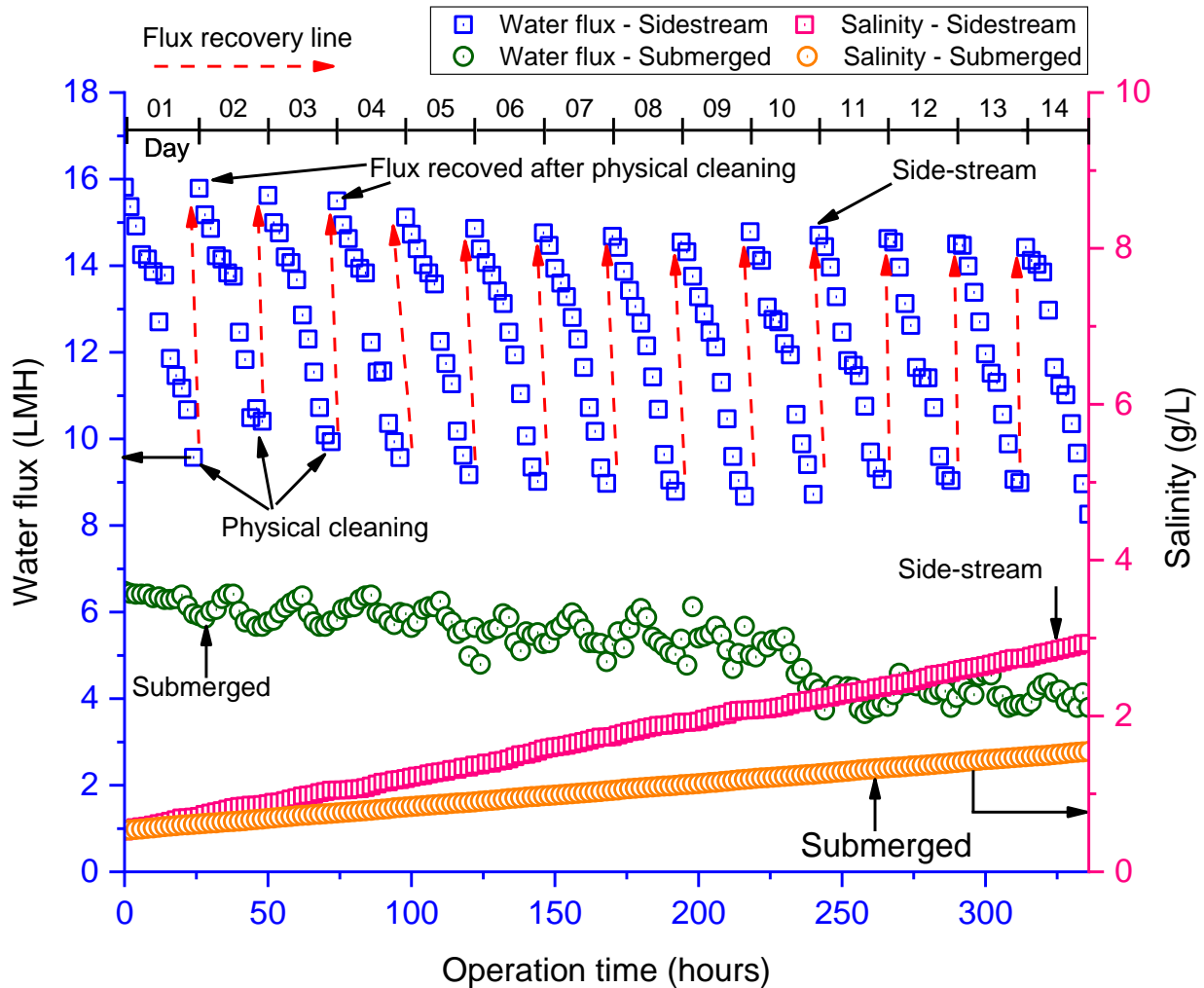
281 Subsequently, continuous aeration with the same intensity as the one used in OMBR systems was
282 sparged into the FS tank to investigate the effect on the performance of the submerged membrane
283 module. As can be seen in **Fig. 2**, interestingly, J_w was only 9.2 LMH, which is 33% lower than
284 without aeration. Under the continuously aerated condition, CECP might have a reduced impact
285 on the performance of the membrane module since aeration generates secondary flows with wakes
286 and shear forces near the membrane surface, destabilizing CECP. Moreover, air bubbles make
287 direct contact, scouring onto the membrane surface, causing hollow fibers to vibrate, thereby
288 mitigating the CECP effect [26]. However, intensive aeration might result in the substantial
289 presence of air bubbles rather than the water on the membrane surface, reducing the contact area

290 between water and membrane surface, deteriorating water flux [25]. This could be the main factor
291 contributing to the lower J_w as aeration was introduced.

292 A lower SRSF value was observed with the side-stream module, which can be ascribed to the
293 combined effect of increased water permeability and hindrance of reverse solute flux (J_s - RSF) in
294 the side-stream system. SRSF is the ratio of J_s over J_w ; SRSF will therefore be lower with a higher
295 J_w . Additionally, reverse diffusion of draw solutes to the FS might also be impeded by the slightly
296 higher hydraulic pressure generated by the recirculation pump on the FS side of the hollow fiber
297 membrane in the side-stream module [9]. The decreased SRSF was in agreement with the findings
298 reported in previous FO study conducted by Morrow et. al [9] and other pressure-assisted forward
299 osmosis research works [27-29].

300

301 3.2 Performance of submerged and side-stream modules in OMBR systems



302
 303 **Figure 3.** Water flux and salinity profiles of the reactor in two submerged and side-stream OMBR
 304 systems. Testing conditions: DS = 35 g/L NaCl; FS = activated sludge; AL – FS orientation;
 305 Ambient temperature ($22 \pm 1^\circ\text{C}$).

306 The profiles of J_w and the bioreactor’s salinity in the submerged and side-stream OMBR systems
 307 over the experiment period are illustrated in **Fig. 3**. Similar to the earlier results from the initial
 308 baseline tests, the side-stream OMBR system produced a much higher J_w when compared to that
 309 of the submerged system. Initial J_w in the crossflow OMBR system was 15.8 LMH, about 2.5 times
 310 higher than that of the submerged OMBR system which demonstrated an initial J_w of 6.5 LMH.

311 The higher J_w in the side-stream system might be due partly to the effect of the slightly higher
312 hydraulic pressure induced by the recirculation pump on the FS side, facilitating the permeation
313 of water to the DS side. Furthermore, the intermittent injection of air bubbles into the side-stream
314 module also likely avoided the presence and direct contact of air bubbles directly on the hollow
315 fiber membrane surface, thereby maintaining the effective membrane surface intact. It is difficult
316 to provide a fair comparison of the effect of CECP between these two systems, however, it is
317 undeniable that wall shear force and the turbulence generated by the circulation with periodic
318 aeration of FS, and continuous aeration in the side-stream module and submerged module,
319 respectively, are different. However, both were found to have positive impacts on alleviating
320 CECP and membrane fouling.

321 The J_w in the side-stream system significantly declined by 40% over 24 hours of operation, while
322 the drop was only 8% for the immersed OMBR system. The difference in the flux decline rate
323 between the two OMBR systems was attributed to the different fouling behaviors and probable
324 intense aeration caused by the different hydrodynamic conditions, such as the initial J_w and aeration
325 rate in these two systems. The rate of membrane fouling was significantly dependent on the initial
326 J_w and as fouling rate was is generally more severe at higher initial J_w values, membranes are
327 generally operated below this critical flux to lower the fouling rate [30]. As a larger volume of
328 water permeates through the membrane, under the effect of convection, more foulants are carried
329 towards the membrane surface, thereby inducing a greater hydrodynamic drag force towards the
330 membrane active surface [31]. Additionally, the side-stream module might have been operated
331 with the initial J_w above the critical flux which perhaps exacerbated the rate of membrane fouling
332 [32].

333 The aeration rate also has considerable influence on fouling tendency of both conventional MBR
334 [26, 33-35] and OMBR systems [15, 21]. Qin et. al [21] reported that for a continuously aerated
335 OMBR system the flux decline was 30% lower compared to an OMBR without aeration. While
336 aeration can help to mitigate membrane fouling, however, intense aeration might unintentionally
337 cause a decrease in the effective membrane area thereby compromising the water flux.

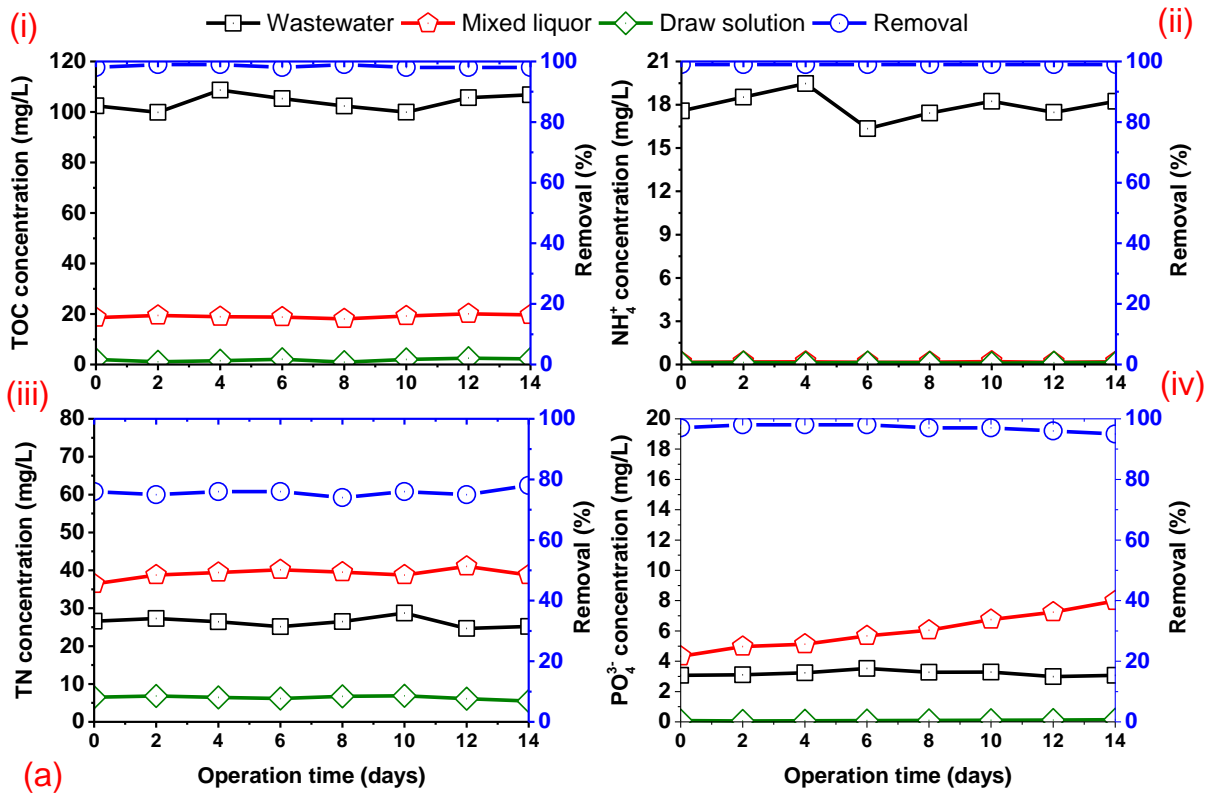
338 Rapid flux decline and high flux recovery happened repeatedly over 14 days of the experimental
339 period for the side-stream OMBR. **Fig 3** shows that the OMBR water almost fully recovered (99%
340 of initial flux) for the side-stream module after physical cleaning at the end of each cycle. The high
341 flux recovery rate in the side-stream system indicates that fouling in this system is reversible, and
342 physical cleaning was effective in mitigating membrane fouling, which agrees well with our
343 previous side-stream OMBR study [15]. Meanwhile, J_w for the submerged OMBR system
344 continuously and slowly decreased without any physical cleaning and this indicates that
345 continuous aeration at an optimum rate could be used as an effective measure of fouling control in
346 a submerged OMBR system.

347 **Fig. 3** also illustrates profiles of the reactor's salinity for the two OMBR systems over the 14-day
348 operation. In general, the salinity of the activated sludge in both OMBR systems successively and
349 slowly increased with a faster build-up rate of the reactor's salinity in the side-stream system. The
350 initial values for the total dissolved solids (TDS) in both systems were comparatively similar at
351 around 0.53 g/L at the beginning, but the salinities of their mixed liquors increased significantly
352 throughout the testing period. The TDS value of activated sludge in the submerged system was
353 almost 2-fold lower than that of the side-stream system at the end of the 14-day operation. This
354 faster rate of draw solute accumulation in the side-stream system might be primarily attributed to
355 the higher J_w of the system. The build-up of salinity in reactors is an unavoidable phenomenon in

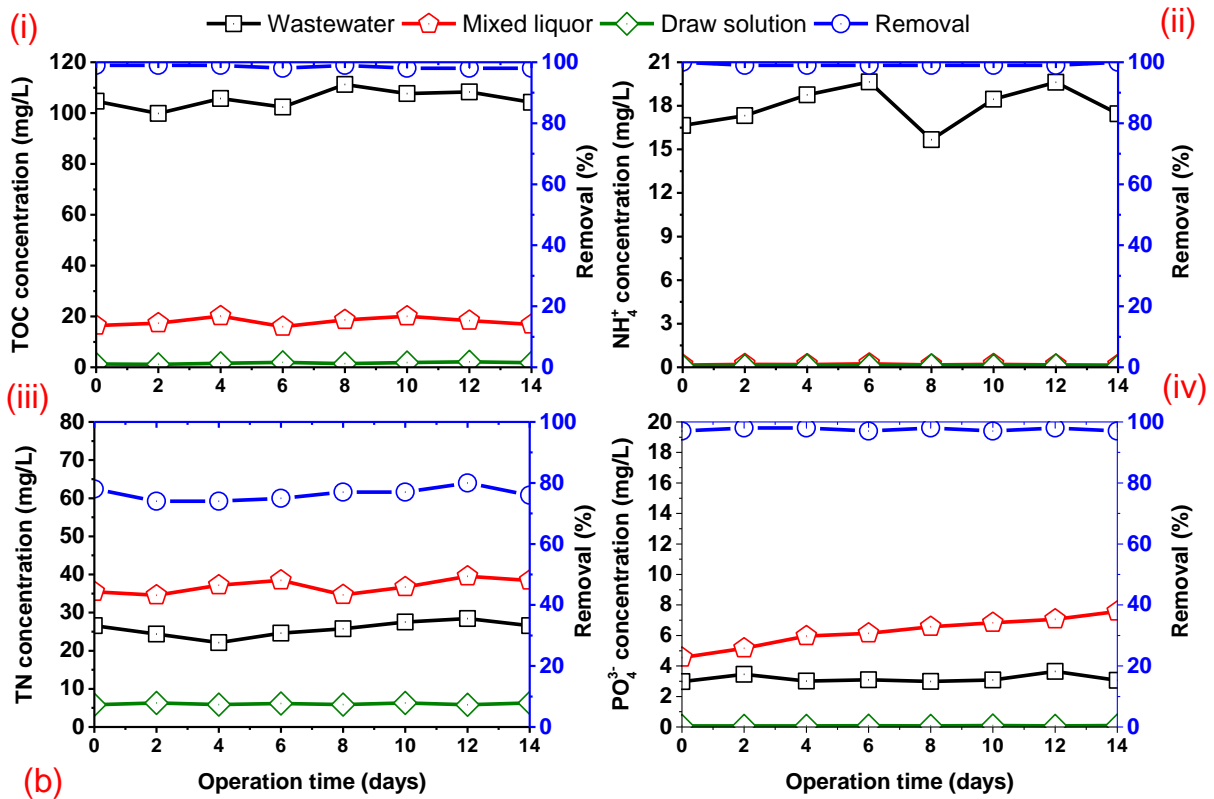
356 any OMBR system, caused by two main factors: cumulative accumulation of rejected feed salt or
 357 brine in the bioreactor as only pure water is drawn out by the high rejection FO membrane, and
 358 partly the reverse diffusion of the draw solute towards the bioreactor feed [3, 8, 14]. The rise in
 359 the reactor's salinity not only lowers the net osmotic driving force, exacerbating the flux decline,
 360 but can also impede the growth and functional activities of microorganisms, deteriorating the
 361 microbiological activities for wastewater treatment [8].

362

363 **3.3 Pollutants removal efficiency**



364



365

366 **Figure 4.** Concentrations and overall pollutant removal efficiencies of (a) the submerged and
 367 side-stream OMBR systems including (i) TOC; (ii) NH_4^+ ; (iii) TN removal; and (iv) PO_4^{3-} .
 368 Testing conditions: DS = 35 g/L NaCl; FS = activated sludge; AL – FS orientation; Ambient
 369 temperature ($22 \pm 1^\circ\text{C}$).

370

371 The removal efficiencies for TOC, ammonium (NH_4^+), total nitrogen (TN), and phosphate (PO_4^{3-})
 372 by the two OMBR systems over the 14-day experiment period are presented in **Fig. 4**. In general,
 373 both the submerged and side-stream OMBR systems exhibited high and stable removal of the four
 374 selected pollutants over the experiment period, with no significant differences in the removal rates.
 375 Synergistic effects between microbial degradation and the high rejection of the FO membrane are
 376 the two main contributors to these high pollutant and nutrient removals from the wastewater [11].

377

378 As shown in Fig. 4a-(i) and Fig. 4b-(i), the two OMBR systems demonstrated consistent TOC
379 removal, over 98% during the 14 day experiment, similar to results observed in previous OMBR
380 studies [14, 15]. Achilli et. al [1] reported a 99% overall TOC removal in their OMBR work while
381 Qiu and Ting [36] noticed a consistent TOC removal efficiency of up to 98%. Some recent OMBR
382 studies have also presented high overall TOC removal with over 98% [37] and 96% [37].

383 Consistently high NH_4^+ removal by the two OMBR systems was also observed over 14 days as
384 illustrated in Fig. 4a-(ii) and Fig. 4b-(ii) which agrees well with our previous OMBR studies using
385 external side-stream modules that reported excellent NH_4^+ removal [14, 15]. Some other OMBR
386 research works have also reported high removal efficacies of NH_4^+ [1, 3, 11, 36]. The high overall
387 NH_4^+ removal by the two OMBR systems is due to the synergistic effects between the biological
388 nitrification by ammonium-oxidizing bacteria and the high rejection of the FO membrane [14].

389 Fig. 4a-(iii) and Fig. 4b-(iii) present the removal rates of TN by the two OMBR systems, which
390 demonstrated consistent removal rates of up to 80% and TN concentrations in the reactors
391 marginally increased over the experiment time. Continuous accumulation of nitrogen compounds
392 in the reactors, which were strongly rejected by the FO membrane, might be attributed to the slight
393 increase of TN concentration in the reactors. Microbial degradation of nitrogen compounds by
394 nitrification and denitrification processes is the main contributor to the TN removal process in the
395 OMBR systems. Nitrification normally is an effective process in the aerobic OMBR system, with
396 sufficient dissolved oxygen, converting ammonium into nitrite and nitrate. However, the
397 denitrification process is not likely to occur in the bioreactor due to the presence of dissolved
398 oxygen and this resulted in the retention and increased accumulation of TN, mostly in the form of
399 nitrates in the bioreactors because of high rejection by FO membrane [38]. Previous OMBR studies

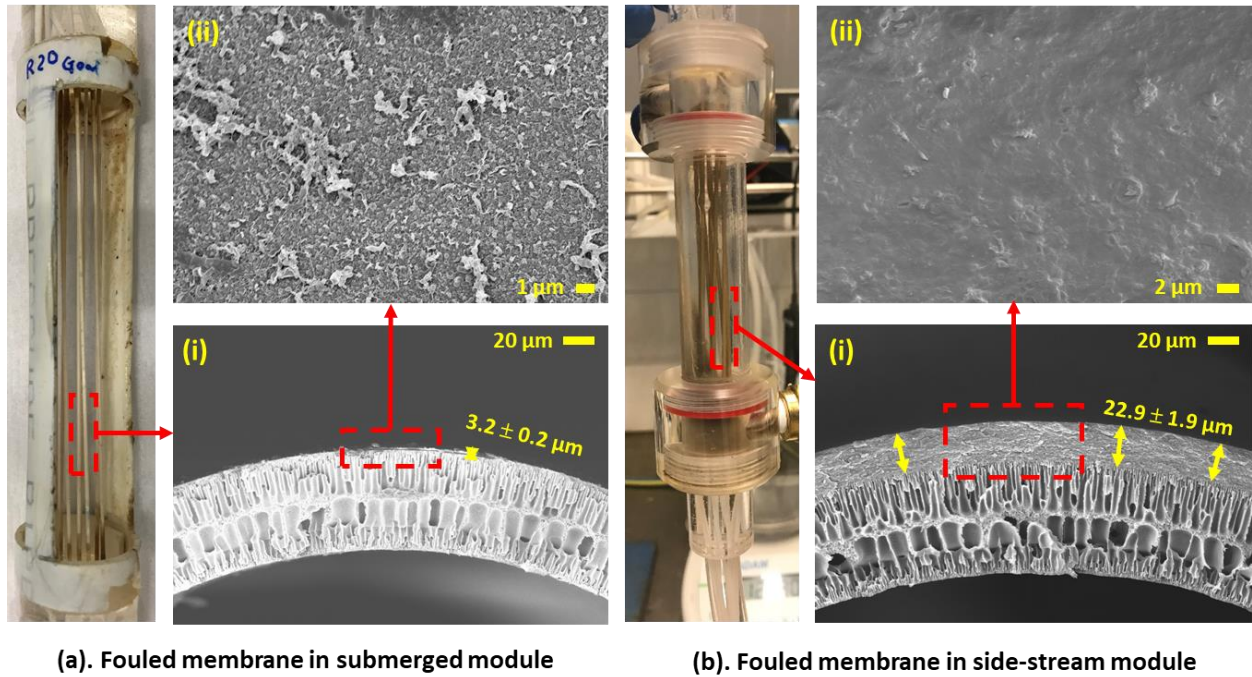
400 using different types of flat-sheet Aquaporin, TFC, and CTA FO membranes also found similar
401 results [3, 19, 39].

402

403 Fig. 4a-(iv) and Fig. 4b-(iv) demonstrate that both OMBR systems achieved consistently high
404 removal of phosphate (PO_4^{3-}), of up to 98%. The high rejection of the FO membrane is expected
405 to be the primary contributor to the effectiveness of PO_4^{3-} . Negatively charged orthophosphate ions
406 have a large hydrated radius diameter of 0.49 nm, which were almost retained by the FO membrane
407 [10]. The high PO_4^{3-} removal rates were in agreement with other OMBR studies that have reported
408 removal rates of 99% and 98% [19]. In conclusion, these two OMBR systems using side-stream
409 and submerged membrane modules with an OSHF TFC FO membrane exhibited stable and high
410 removal efficacies of the four investigated pollutants.

411

412 **3.4 Membrane and fouling cake layer characterization.**



413 (a). Fouled membrane in submerged module (b). Fouled membrane in side-stream module
 414 **Figure 5.** SEM images of fouled OSHF TFC FO membranes (without cleaning) in (a) submerged
 415 module and (b) side-stream module; (i) cross-sectional morphology; and (ii) outer surface
 416 morphology.

417 **Table 1** The elemental compositions of pristine and fouled membranes in two operation regimes
 418 by energy-dispersive X-ray (EDX) analysis.
 419
 420

Weight %	C	O	N	S	Na	Cl	Mg	Al	Si	P	Ca	Fe
Submerged	55.42	17.56	4.75	3.08	6.24	8.15	0.24	0.35	0.19	1.15	1.02	1.85
Side-stream	47.21	15.34	5.94	4.24	7.34	10.46	0.93	0.96	0.73	2.34	1.95	2.56

421
 422 Fig. 5 shows images of submerged and side-stream membrane modules and SEM images of the
 423 outer surface and cross-sectional morphologies of fouled hollow fiber FO membrane at the end of
 424 the experiment period without washing. Cross-sectional SEM images in Fig. 5a-(i) and Fig. 5b-(i)
 425 demonstrate the significant difference in thickness for the fouling cake layers. The thickness of the
 426 cake layer of a fouled membrane in the side-stream module was found to be $22.9 \pm 1.9 \mu\text{m}$, 7-fold

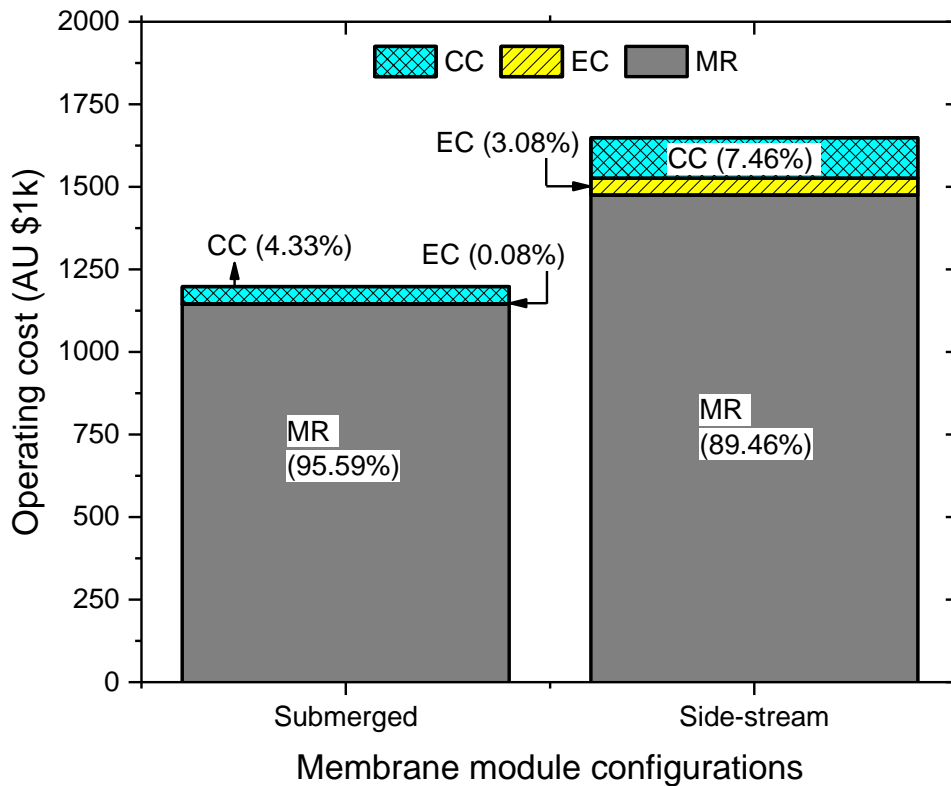
427 thicker than the one in submerged module, with a thickness of $3.2 \pm 0.2 \mu\text{m}$. The outer surface
428 morphologies shown Fig. 5a-(ii) and Fig. 5b-(ii) further confirm that the outer surface of the fouled
429 hollow membrane in the side-stream module was completely covered by a dense and thick foulant
430 layer. However, only a small portion of the outer surface of the fouled membrane in the submerged
431 module was covered by foulants. There was a large area with typical ridge-and-valley morphology
432 of the polyamide selective layer that can be visually seen on the outer surface of the fouled
433 membrane in the submerged module that was not observed for the side-stream membrane. This
434 result is in contrast to the one observed by Morrow et. al [9] in their OMBR study in which they
435 reported that the cake layer of a fouled flat-sheet CTA membrane in the submerged module was
436 thicker than the one in the side-stream configuration.

437 The scattering of foulants on the outer surface of the fouled submerged hollow fibre membrane
438 indicates that foulants could not be deposited onto the membrane surface under continuous aeration
439 in this study. The direct contact of air bubbles onto the membrane surface generated air scouring
440 and hindered the initial interaction between foulants and the membrane surface, inhibiting
441 subsequent foulant-foulant interactions need to form a thicker cake layer. This finding confirms
442 why the flux decline rate in the submerged OMBR system was significantly slower when
443 compared to the side-stream module. Similarly, previous research studies on conventional
444 submerged MBR and OMBR systems reported the effectiveness of air bubbles as a fouling control
445 method [35, 40-42].

446 The elemental compositions of the fouling cake layers taken from the two membrane modules
447 were analyzed using EDX. According to the analytical results presented in Table 1, both fouling
448 cake layers contained various inorganic elements including Na, Cl, Mg, Al, Si, P, Ca, and Fe, and
449 four main elements (C, O, N, and S) that come from the functional groups of the FO membrane

450 itself. Results in Table 1 also show that the fouled membrane from the side-stream module
 451 contained higher percentages of the analyzed elements than the one in the submerged module. This
 452 is a reasonable, as the fouling cake layer in the side-stream module was thicker and more
 453 compacted with foulants. The presence of Ca, Mg, and Si might be an indicator of inorganic scaling
 454 in addition to organic and biofouling, and other elements such as Fe and P might originally come
 455 from the synthetic wastewater. A high amount of Na and Cl detected in the fouling cake layer
 456 could be related to the reversely diffused draw solutes which accumulated in the fouling cake layer.

457 **3.5 Operating costs comparison between submerged and side-stream module configurations**



458

459 **Figure 6.** Annual OPEXs and cost contributions of membrane replacement (MR), energy
460 consumption (EC), and cleaning cost (CC) to operating costs (OPEX) of the submerged and side-
461 stream OMBR systems for a plant capacity of 24,000 m³/day.

462 **Fig. 6** presents the annual operating costs (OPEX) and cost contributions of the three main
463 operating components, including membrane replacement (MR), energy consumption (EC), and
464 cleaning cost (CC) to the overall OPEX of the submerged and side-stream OMBR systems. In
465 general, the submerged OMBR system demonstrated a lower operating cost (AU \$1.20 million per
466 annum) than that of the side-stream OMBR system (AU \$1.65 million per annum) to produce a
467 similar volume of diluted DS. This result demonstrates that the submerged OMBR system is more
468 economically viable compared to the side-stream system. MR was the major cost contributor,
469 while the EC and CC were relatively minor ones for the two OMBR systems. The cost of MR in
470 the side-stream system was AU \$1.48 million, accounting for 89.46% of the OPEX, which is 1.29
471 times higher the MR cost (AU \$1.14 million – 95.59%) for the submerged system. This is mainly
472 due to the lower cost of the submerged membrane module even the submerged system requires
473 double the number of membrane modules compared to the side-stream to produce a similar volume
474 of diluted DS. The higher cost of the side-stream membrane module is due to the additional cost
475 of housing materials and increased complexity in its production.

476 EC and CC in the submerged OMBR system were much lower than that of the side-stream system.
477 For instance, EC cost contributed only 0.08% to the overall OPEX of the submerged system, which
478 is 50 times lower than that of the side-stream system, contributing 3.08% to the overall OPEX.
479 The main reason for this difference is that the side-stream OMBR system requires much more
480 power for the circulation of mixed liquor into the cross-flow membrane module, and the regular
481 injection of air bubbles into the membrane module, while there was no recirculation of activated

482 sludge carried out in the submerged OMBR system. Similarly, the CC in the immersed system
483 contributed 4.33% to the overall OPEX, which is two-fold lower than CC cost for the side-stream
484 system, which accounted for 7.46% of its overall OPEX. This is due to the higher frequency of
485 physical and chemical cleaning required for the cross-flow modules compared to the submerged
486 ones, even though the number of submerged modules was almost double.

487 Results of the economic analysis demonstrate that the submerged OMBR system is more viable
488 when compared to the side-stream. Further, the utilization of submerged membrane modules does
489 not require circulation of activated sludge, which will minimize harmful impacts on the growth
490 and biodegradation activities of microorganism. Circulation of activated sludge with high CFV
491 generates strong shear force resulting in detrimental damage and breakage of microbial flocs,
492 lower sludge yield, and reduced removal efficiency of pollutants [20]. Furthermore, more fine
493 colloidal particles are created with the breakages of flocs, which releases extracellular polymeric
494 substances (EPS), increasing the resistance of the fouling cake layer, exacerbating membrane
495 fouling. The submerged OMBR system is therefore more preferable for a long-term operation as
496 it has can sustain its flux for longer periods. However, to make the submerged system more viable,
497 a reduction in OPEX cost is required. Based on the OPEX cost components of the two OMBR
498 systems, the most direct way is to lower the cost of MR. Logically, the two obvious approaches
499 to lower the MR cost is to develop OHF FO membranes with better performance in terms of water
500 flux and fouling control [24]. While membrane price depends upon the market's maturity and
501 mass production, higher water flux can be achieved by optimizing operating conditions and using
502 new generations of membrane modules possessing better properties.

503

504

505 4 Conclusions

506 This study conducted an evaluation of the comparative performances of two different OMBR
507 module configurations (submerged and side-stream) using an outer-selective hollow fiber thin-
508 film composite forward osmosis membrane in terms of their fouling potential and fouling
509 mitigation efficiencies. In general, the cross-flow side-stream OMBR module demonstrated a
510 higher water flux but experienced more severe fouling compared to the submerged membrane
511 module, thereby requiring more frequent physical cleaning. Both the OMBR systems, however,
512 achieved similarly high removal efficiencies of both pollutants and nutrients (TOC, NH_4^+ , TN, and
513 PO_4^{3-}) over the entire experimental period. Normal aeration used in the bioreactor can also be
514 utilized as an effective fouling mitigation method in the submerged OMBR system without the
515 need for additional aeration as a fouling control. The submerged OMBR system demonstrated
516 lower OPEX cost compared to the side-stream system and membrane replacement cost formed
517 major cost component of the both the OMBR systems. Therefore, employing higher performance
518 outer selective hollow fiber FO membrane and low-cost submerged module will reduce the OPEX
519 cost of the OMBR system.

520

521 Acknowledgments

522 This work was supported by the Australian Research Council (ARC) Industrial Transformation
523 Research Hub (IH170100009), the Qatar National Research Fund (QNRF) [NPRP 9-052-2-020]
524 and the Hong Kong Special Administrative Region, China (Project No. T21-604/19-R).

525

526 References

- 528 [1] A. Achilli, T.Y. Cath, E.A. Marchand, A.E. Childress, The forward osmosis membrane
529 bioreactor: A low fouling alternative to MBR processes, *Desalination*, 239 (2009) 10-21.
- 530 [2] G. Blandin, C. Gautier, M. Sauchelli Toran, H. Monclús, I. Rodriguez-Roda, J. Comas,
531 Retrofitting membrane bioreactor (MBR) into osmotic membrane bioreactor (OMBR): A
532 pilot scale study, *Chem. Eng. J.*, 339 (2018) 268-277.
- 533 [3] W. Luo, H.V. Phan, M. Xie, F.I. Hai, W.E. Price, M. Elimelech, L.D. Nghiem, Osmotic
534 versus conventional membrane bioreactors integrated with reverse osmosis for water reuse:
535 Biological stability, membrane fouling, and contaminant removal, *Water Res.*, 109 (2017)
536 122-134.
- 537 [4] B. Yuan, X. Wang, C. Tang, X. Li, G. Yu, In situ observation of the growth of
538 biofouling layer in osmotic membrane bioreactors by multiple fluorescence labeling and
539 confocal laser scanning microscopy, *Water Res.*, 75 (2015) 188-200.
- 540 [5] B. Wu, T. Kitade, T.H. Chong, T. Uemura, A.G. Fane, Impact of membrane bioreactor
541 operating conditions on fouling behavior of reverse osmosis membranes in MBR-RO
542 processes, *Desalination*, 311 (2013) 37-45.
- 543 [6] M. Pontié, S. Rapenne, A. Thekkedath, J. Duchesne, V. Jacquemet, J. Leparç, H. Suty,
544 Tools for membrane autopsies and antifouling strategies in seawater feeds: a review,
545 *Desalination*, 181 (2005) 75-90.
- 546 [7] W. Luo, B. Arhatari, S.R. Gray, M. Xie, Seeing is believing: Insights from synchrotron
547 infrared mapping for membrane fouling in osmotic membrane bioreactors, *Water Res.*, 137
548 (2018) 355-361.
- 549 [8] R.W. Holloway, A. Achilli, T.Y. Cath, The osmotic membrane bioreactor: a critical
550 review, *Environ. Sci.: Water Res. Technol.*, 1 (2015) 581-605.
- 551 [9] C.P. Morrow, A.L. McGaughey, S.R. Hiibel, A.E. Childress, Submerged or sidestream?
552 The influence of module configuration on fouling and salinity in osmotic membrane
553 bioreactors, *J. Membr. Sci.*, 548 (2018) 583-592.
- 554 [10] N. Pathak, L. Chekli, J. Wang, Y. Kim, S. Phuntsho, S. Li, N. Ghaffour, T. Leiknes,
555 H. Shon, Performance of a novel baffled osmotic membrane bioreactor-microfiltration
556 hybrid system under continuous operation for simultaneous nutrient removal and
557 mitigation of brine discharge, *Bioresour. Technol.*, 240 (2017) 50-58.
- 558 [11] N. Pathak, S. Li, Y. Kim, L. Chekli, S. Phuntsho, A. Jang, N. Ghaffour, T. Leiknes,
559 H.K. Shon, Assessing the removal of organic micropollutants by a novel baffled osmotic
560 membrane bioreactor-microfiltration hybrid system, *Bioresour. Technol.*, 262 (2018) 98-
561 106.
- 562 [12] S. Phuntsho, J.E. Kim, V.H. Tran, S. Tahara, N. Uehara, N. Maruko, H. Matsuno, S.
563 Lim, H.K. Shon, Free-standing, thin-film, symmetric membranes: Next-generation
564 membranes for engineered osmosis, *J. Membr. Sci.*, 607 (2020) 118145.
- 565 [13] J. Zhang, W.L.C. Loong, S. Chou, C. Tang, R. Wang, A.G. Fane, Membrane
566 biofouling and scaling in forward osmosis membrane bioreactor, *J. Membr. Sci.*, 403-404
567 (2012) 8-14.

568 [14] V.H. Tran, S. Lim, D.S. Han, N. Pathak, N. Akther, S. Phuntsho, H. Park, H.K. Shon,
569 Efficient fouling control using outer-selective hollow fiber thin-film composite membranes
570 for osmotic membrane bioreactor applications, *Bioresour. Technol.*, 282 (2019) 9-17.

571 [15] V.H. Tran, S. Lim, M. Jun Park, D. Suk Han, S. Phuntsho, H. Park, H. Matsuyama, H.
572 Kyong Shon, Fouling and performance of outer selective hollow fiber membrane in
573 osmotic membrane bioreactor: Cross flow and air scouring effects, *Bioresour. Technol.*,
574 295 (2020) 122303.

575 [16] S. Lim, N. Akther, V.H. Tran, T.-H. Bae, S. Phuntsho, A. Merenda, L.F. Dumée, H.K.
576 Shon, Covalent organic framework incorporated outer-selective hollow fiber thin-film
577 nanocomposite membranes for osmotically driven desalination, *Desalination*, 485 (2020)
578 114461.

579 [17] S. Lim, K.H. Park, V.H. Tran, N. Akther, S. Phuntsho, J.Y. Choi, H.K. Shon, Size-
580 controlled graphene oxide for highly permeable and fouling-resistant outer-selective
581 hollow fiber thin-film composite membranes for forward osmosis, *J. Membr. Sci.*, 609
582 (2020) 118171.

583 [18] V.H. Tran, S. Phuntsho, D.S. Han, U. Dorji, X. Zhang, H.K. Shon, Submerged module
584 of outer selective hollow fiber membrane for effective fouling mitigation in osmotic
585 membrane bioreactor for desalination, *Desalination*, 496 (2020) 114707.

586 [19] N.C. Nguyen, S.-S. Chen, H.T. Nguyen, S.S. Ray, H.H. Ngo, W. Guo, P.-H. Lin,
587 Innovative sponge-based moving bed–osmotic membrane bioreactor hybrid system using
588 a new class of draw solution for municipal wastewater treatment, *Water Res.*, 91 (2016)
589 305-313.

590 [20] J.-S. Kim, C.-H. Lee, I.-S. Chang, Effect of pump shear on the performance of a
591 crossflow membrane bioreactor, *Water Res.*, 35 (2001) 2137-2144.

592 [21] J.-J. Qin, K.A. Kekre, M.H. Oo, G. Tao, C.L. Lay, C.H. Lew, E.R. Cornelissen, C.J.
593 Ruiken, Preliminary study of osmotic membrane bioreactor: effects of draw solution on
594 water flux and air scouring on fouling, *Water Sci. Technol.*, 62 (2010) 1353-1360.

595 [22] S. Lim, V.H. Tran, N. Akther, S. Phuntsho, H.K. Shon, Defect-free outer-selective
596 hollow fiber thin-film composite membranes for forward osmosis applications, *J. Membr.*
597 *Sci.*, 586 (2019) 281-291.

598 [23] A. APHA, WEF, Standard methods for the examination of water and wastewater,
599 American Public Health Association (APHA): Washington, DC, USA, (2005).

600 [24] J.E. Kim, S. Phuntsho, L. Chekli, S. Hong, N. Ghaffour, T. Leiknes, J.Y. Choi, H.K.
601 Shon, Environmental and economic impacts of fertilizer drawn forward osmosis and
602 nanofiltration hybrid system, *Desalination*, 416 (2017) 76-85.

603 [25] G. Blandin, I. Rodriguez-Roda, J. Comas, Submerged Osmotic Processes: Design and
604 Operation to Mitigate Mass Transfer Limitations, *Membranes*, 8 (2018) 72.

605 [26] R. Ghosh, Enhancement of membrane permeability by gas-sparging in submerged
606 hollow fibre ultrafiltration of macromolecular solutions: Role of module design, *J. Membr.*
607 *Sci.*, 274 (2006) 73-82.

608 [27] G. Blandin, A.R.D. Verliefde, C.Y. Tang, A.E. Childress, P. Le-Clech, Validation of
609 assisted forward osmosis (AFO) process: Impact of hydraulic pressure, *J. Membr. Sci.*, 447
610 (2013) 1-11.

611 [28] B.D. Coday, D.M. Heil, P. Xu, T.Y. Cath, Effects of Transmembrane Hydraulic
612 Pressure on Performance of Forward Osmosis Membranes, *Environ. Sci. Technol.*, 47
613 (2013) 2386-2393.

614 [29] Y. Oh, S. Lee, M. Elimelech, S. Lee, S. Hong, Effect of hydraulic pressure and
615 membrane orientation on water flux and reverse solute flux in pressure assisted osmosis, *J.*
616 *Membr. Sci.*, 465 (2014) 159-166.

617 [30] Y. Kim, S. Lee, H.K. Shon, S. Hong, Organic fouling mechanisms in forward osmosis
618 membrane process under elevated feed and draw solution temperatures, *Desalination*, 355
619 (2015) 169-177.

620 [31] Q. She, R. Wang, A.G. Fane, C.Y. Tang, Membrane fouling in osmotically driven
621 membrane processes: A review, *J. Membr. Sci.*, 499 (2016) 201-233.

622 [32] T.-T. Nguyen, S. Kook, C. Lee, R.W. Field, I.S. Kim, Critical flux-based membrane
623 fouling control of forward osmosis: Behavior, sustainability, and reversibility, *J. Membr.*
624 *Sci.*, 570-571 (2019) 380-393.

625 [33] J.-y. Tian, Y.-p. Xu, Z.-l. Chen, J. Nan, G.-b. Li, Air bubbling for alleviating
626 membrane fouling of immersed hollow-fiber membrane for ultrafiltration of river water,
627 *Desalination*, 260 (2010) 225-230.

628 [34] K. Zhang, P. Wei, M. Yao, R.W. Field, Z. Cui, Effect of the bubbling regimes on the
629 performance and energy cost of flat sheet MBRs, *Desalination*, 283 (2011) 221-226.

630 [35] F. Wicaksana, A.G. Fane, V. Chen, Fibre movement induced by bubbling using
631 submerged hollow fibre membranes, *J. Membr. Sci.*, 271 (2006) 186-195.

632 [36] G. Qiu, Y.-P. Ting, Osmotic membrane bioreactor for wastewater treatment and the
633 effect of salt accumulation on system performance and microbial community dynamics,
634 *Bioresour. Technol.*, 150 (2013) 287-297.

635 [37] W. Zhu, X. Wang, Q. She, X. Li, Y. Ren, Osmotic membrane bioreactors assisted with
636 microfiltration membrane for salinity control (MF-OMBR) operating at high sludge
637 concentrations: Performance and implications, *Chem. Eng. J.*, 337 (2018) 576-583.

638 [38] P. Jin, Y. Chen, T. Xu, Z. Cui, Z. Zheng, Efficient nitrogen removal by simultaneous
639 heterotrophic nitrifying-aerobic denitrifying bacterium in a purification tank bioreactor
640 amended with two-stage dissolved oxygen control, *Bioresour. Technol.*, 281 (2019) 392-
641 400.

642 [39] W. Luo, M. Xie, X. Song, W. Guo, H.H. Ngo, J.L. Zhou, L.D. Nghiem, Biomimetic
643 aquaporin membranes for osmotic membrane bioreactors: Membrane performance and
644 contaminant removal, *Bioresour. Technol.*, 249 (2018) 62-68.

645 [40] B.D. Coday, P. Xu, E.G. Beaudry, J. Herron, K. Lampi, N.T. Hancock, T.Y. Cath,
646 The sweet spot of forward osmosis: Treatment of produced water, drilling wastewater, and
647 other complex and difficult liquid streams, *Desalination*, 333 (2014) 23-35.

648 [41] A. Drews, H. Prieske, E.-L. Meyer, G. Senger, M. Kraume, Advantageous and
649 detrimental effects of air sparging in membrane filtration: Bubble movement, exerted shear
650 and particle classification, *Desalination*, 250 (2010) 1083-1086.

651 [42] G. Ducom, F.P. Puech, C. Cabassud, Air sparging with flat sheet nanofiltration: a link
652 between wall shear stresses and flux enhancement, *Desalination*, 145 (2002) 97-102.

653

Elsevier required licence: © 2021

This manuscript version is made available under the
CC-BY-NC-ND 4.0 license

<http://creativecommons.org/licenses/by-nc-nd/4.0/>

The definitive publisher version is available online at

<https://doi.org/10.1016/j.desal.2021.115196>